NOTES AND CORRESPONDENCE

Wind Energy Input to the Surface Waves*

WEI WANG

Physical Oceanography Laboratory, Ocean University of China, Qingdao, Shandong, China

RUI XIN HUANG

Department of Physical Oceanography, Woods Hole Oceanographic Institution, Woods Hole, Massachusetts

2 January 2003 and 29 October 2003

ABSTRACT

Wind energy input into the ocean is primarily produced through surface waves. The total rate of this energy source, integrated over the World Ocean, is estimated at 60 TW, based on empirical formulas and results from a numerical model of surface waves. Thus, surface wave energy input is about 50 times the energy input to the surface geostrophic current and 20 times the total tidal dissipation rate. Most of the energy input is concentrated within the Antarctic Circumpolar Current.

1. Introduction

Mechanical energy input through wind stress is the most important component of energetics of the global oceans. Faller (1966) made an attempt to estimate mechanical energy sources of the World Ocean, including wind stress, tidal dissipation, and other terms. Lueck and Reid (1984) estimated that the total amount of downward mechanical energy flux in the atmospheric boundary layer is about 510 TW, and ''about 2–10% of this downward energy flux eventually enters the ocean.'' Thus far, there has been no reliable estimate of the total energy input from wind stress.

Using satellite data and a numerical model, wind energy input through the surface geostrophic current is estimated at 1.3 TW (Wunsch 1998). Wind stress energy input through the surface ageostrophic current consists of two parts: 1) Near-inertial motions are approximately 0.5–0.7 TW as estimated by Watanabe and Hibiya (2002) and Alford (2003) (although these authors seem to be in dispute, the difference in the energy estimate is small). 2) The contribution for subinertial motions is estimated at 2.4 TW (Wang and Huang 2004). Thus, the total amount of wind energy input through the surface Ekman drift is about 3 TW.

The most important term is through surface waves. Many papers and books have been published about surface waves (e.g., Phillips 1977), including in situ and laboratory observations, theoretical studies, and numerical simulations. Energetics of surface waves is one of the most important aspects of surface waves. Nevertheless, there has been no estimate of the total energy input for global oceans. Our goal in this study is to estimate wind stress energy input to surface waves in the World Ocean.

2. Energy input to the surface waves

Wind energy input to surface waves can be estimated by the following formula (Gemmrich et al. 1994):

$$W_{\text{waves}} = \tau\overline{c} = \rho_a u_{*a}^2 \overline{c} \approx \rho_w u_{*w}^2 \overline{c}, \qquad (1)$$

where $\overline{c}$ is the effective phase speed, $u_{*a} = \sqrt{\tau/\rho_a}$ and $u_{*w} = \sqrt{\tau/\rho_w}$, ρ_a and ρ_w are density of air and water, and τ is stress at the air–sea interface.

Using data collected through the Water–Air Vertical Exchange Studies (WAVES) experiment, Terray et al. (1996; their Table 1) calculated the corresponding value of $\overline{c}$. This set of data corresponds to waves of a relatively young age, $4.3 < c_{p*} < 7.4$, where $c_{p*} = c_p/u_{*a}$ is the wave age and c_p is the phase velocity at the wind-sea peak frequency. Drennan et al. (1996; their Table 1) used data collected through the Surface Waves Dynamics Experiment (SWADE) to obtain another set of $\overline{c}$.

* Woods Hole Oceanographic Institution Contribution Number 10888.

Corresponding author address: R. X. Huang, Department of Physical Oceanography, Woods Hole Oceanographic Institution, Woods Hole, MA 02543.
E-mail: rhuang@whoi.edu

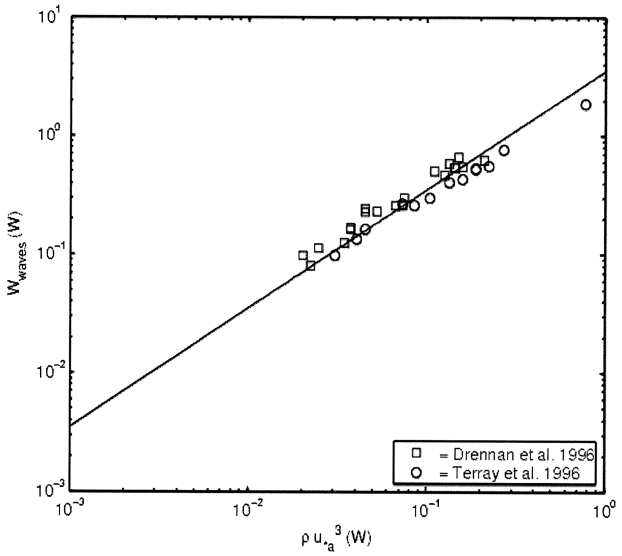

FIG. 1. The wind stress energy input into surface waves.

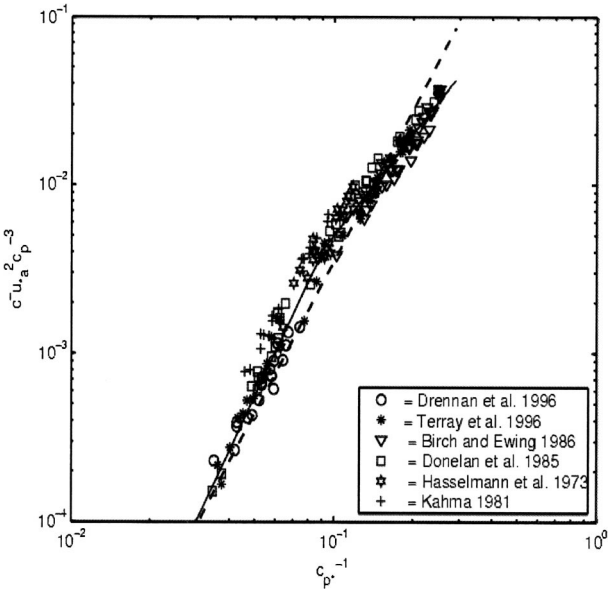

FIG. 2. The correlation between $\overline{c}u^2_{*a}/c_p^3$ and u_{*a}/c_p.

This set of data corresponds to nearly mature waves, $13.5 < c_{p*} < 28.6$. Thus, these two sets of data represent good coverage of wave age, with a gap at $7.4 < c_{p*} < 13.5$.

The rate of wind energy input W_{waves} for these two experiments, WAVES and SWADE, versus $\rho_a u_{*a}^3$ is plotted in Fig. 1. These data can be closely fitted with a straight line,

$$W_{\text{waves}} = 3.5\rho_a u_{*a}^3, \tag{2}$$

within mean relative errors of 16% (WAVES) and 20% (SWADE), respectively.

Because u_{*a} depends not only on wind but also on sea state (Terray 1996), the influence of waves on W_{waves} is implicitly implied in (2). On the other hand, many existent empirical formulas of u_{*a} depend on wind speed only and can give rise to acceptable results (Wu 1982; Watanabe and Hibiya 2002); thus, according to (2), the effect of sea state on W_{waves} may be relatively weak. The insensitivity of energy flux to sea state was also found by Craig and Banner (1994), when dealing with sea surface dynamical processes, using a ''level 2½'' turbulence closure scheme.

In addition, the energy flux factor $\overline{c}/u_{*a}$ depends on wave ages. Scaling values from Fig. 6 of Terray et al. (1996), which shows the relation of $\overline{c}/c_p$ and u_{*a}/c_p, produced a relation between $\overline{c}u_{*a}^3/c_p^3$ and u_{*a}/c_p, as shown in Fig. 2. Because $\overline{c}u_{*a}^2/c_p^3 = W_{\text{waves}}/\rho_a c_p^3$, this figure can be used to infer the relation between W_{waves} and c_{p*}. The mean relative errors between the observation data and (2) (indicated by dashed line) are 20%–65% for the first five datasets listed in the figure and 120% for the last one.

To get the best fit of the experimental data in Fig. 2, we suggest an empirical formula

$$W_{\text{waves}} = A\rho_a u_{*a}^3, \tag{3}$$

where A is the empirical coefficient representing the energy flux factor $\overline{c}/u_{*a}$:

$$A = \begin{cases} 0.5c_{p*}, & \text{as } c_{p*} \le 11 \\ 12c_{p*}^{-1/3}, & \text{as } c_{p*} > 11, \end{cases} \tag{4}$$

indicated in Fig. 2 by the bent solid line.

It is clear that (3) and (4) fit the experimental data better than (2), and the mean relative errors are reduced to about 15%–24% for the first five datasets and 60% for the last one listed in Fig. 2.

However, it is difficult to measure the value of c_{p*}. Thus, two other parameters, the nondimensional spectral peak wave period $T_{p*} = T_p g/u_{*a}$ and the nondimensional significant wave height $H_* = H_s g/u_{*a}^2$, can be used, where T_p is spectral peak wave period, H_s is significant wave height, and g is the gravitational acceleration.

For deep-water waves, the dispersion relation is $\omega = gk$, where k is the wavenumber, and the relation between c_{p*} and T_{p*} is $c_{p*} = (1/2\pi)T_{p*}$; thus, the wind energy flux factor is

$$A = \begin{cases} \dfrac{1}{4\pi}T_{p*}, & \text{as } T_{p*} < 70 \\ 22T_{p*}^{-1/3}, & \text{as } T_{p*} > 70. \end{cases} \tag{5}$$

The wave age c_{p*} and the nondimensional significant wave height H_* are related through $H_* = c_{p*}^{2/3}$ (Toba 1974; Maat et al. 1991), and so we have the relation between A and H_*:

$$A = \begin{cases} 0.5H_*^{2/3}, & \text{as } H_* \le 36 \\ 12H_*^{-2/9}, & \text{as } H_* > 36. \end{cases} \tag{6}$$

TABLE 1. Wind energy input into surface waves for the period Jul 1997–Jun 2002 (TW). The asterisks in the bottom row indicate estimations that assume the ratio between the second and third rows in the second column remain the same for columns three and four.

Eqs.	(2), (7)	(5), (7)	(6), (7)	Avg
78°S–78°N	52.4	54.9	57.1	
90°S–90°N	57.4	60.2*	62.2*	60

3. Wind energy input to surface waves for the global oceans

a. Data selection

Using different formulas for calculating the wind energy input to the surface waves discussed above requires data from wind stress, significant wave height, spectral peak period, and wave age. In this study we use the daily-mean wind stress of National Oceanic and Atmospheric Administration (NOAA)/National Centers for Environmental Prediction (NCEP)–National Center for Atmospheric Research data from 1948 to 2002. These wind stress data have a zonally uniform spacing of 1.875° and a meridionally nonuniform spacing that varies from 1.89° at the Poles to 2.1° near the equator.

Calculation depending on the surface wave is based on the output from a NOAA/NCEP ''WAVEWATCH III,'' global surface wave model. The corresponding data cover the period from 1 July 1997 to 30 June 2002. The temporal resolution is 3 h, and the spatial resolution is 1.25°. This data set covers the latitudinal band of 78°S–78°N. Because the Arctic is relatively small and is covered by sea ice for a substantial part of a year, wind energy input to that part of the World Ocean is a relatively small portion of the global budget. To match the wind stress data, the surface wave data are averaged for each day and interpolated to the same grids as the wind stress data.

b. Calculations

Wind energy to surface waves is calculated in two ways:

1) QUASI-STEADY CALCULATION

The annual mean wind energy input to the surface waves is defined as the mean of the energy input based on daily mean wind stress; that is,

$$W_{\text{waves}} = \frac{1}{N}\sum_{i}^{N} w_{\text{waves},i}, \tag{7}$$

where N is the total number of days of wind stress data and $w_{\text{waves},I}$, is the wind energy input for the ith day.

2) SPECTRAL DISTRIBUTION OF ENERGY

It is useful to explore the spectral distribution of wind energy input to surface waves. First, wind stress can be expanded into the Fourier series

$$\boldsymbol{\tau}(t) = \sum_{n=0}^{N} T_n e^{i\omega_n t},$$

where

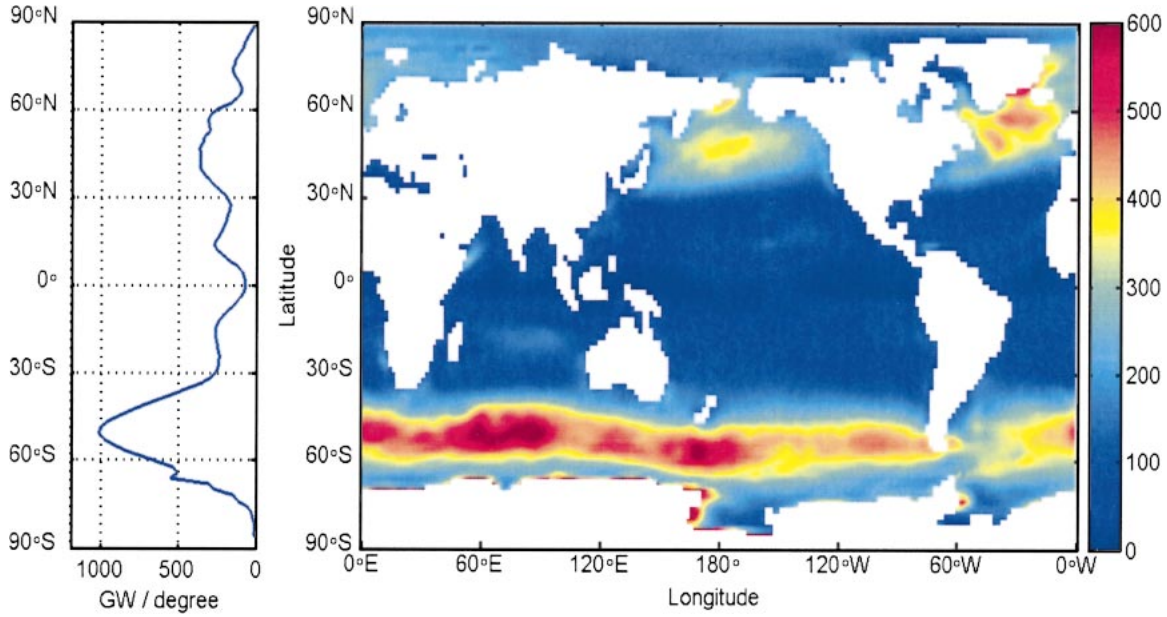

FIG. 3. (right) Distribution of wind stress work on the surface waves (mW m^{-2}) calculated from (2) and (7), and (left) its latitudinal distribution.

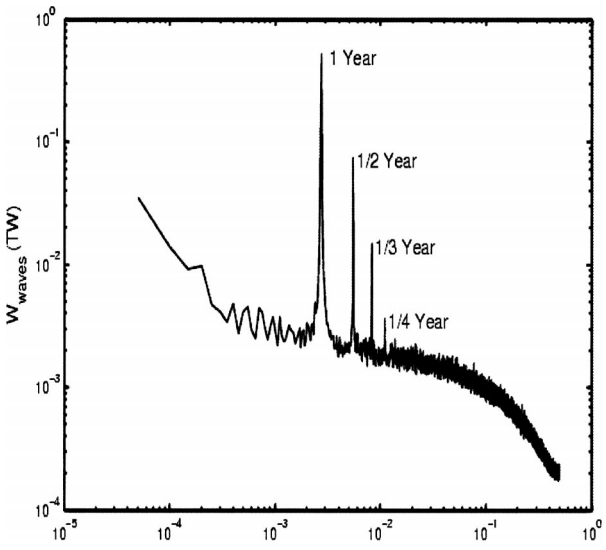

FIG. 4. Distribution of wind stress work on different frequencies (TW), calculated from (11).

$$T_n = T_{x,n} + iT_{y,n} \quad \text{and} \quad \omega_n = \frac{2\pi n}{N}. \tag{8}$$

Wind energy input into surface waves is

$$W_{\text{waves}} = \boldsymbol{\tau}(t) \cdot \mathbf{C}(t), \tag{9}$$

where

$$\mathbf{C}(t) = \frac{A\boldsymbol{\tau}(t)}{\rho_a \overline{u}_*} \tag{10}$$

and $\overline{u}_*$ is the mean friction velocity at a given station. Wind stress energy input corresponding to the nth component is

$$w_{\text{waves}} = \frac{A}{\rho_a \overline{u}_*} T_n^2,$$

where

$$T_n^2 = T_{x,n}^2 + T_{y,n}^2,$$

and the rate of energy input is

$$W_{\text{waves}} = \sum_{n=0}^{N} w_{\text{waves},n} = \sum_{n=0}^{N} \frac{A}{\rho_a \overline{u}_*} T_n^2. \tag{11}$$

These formulas were used to estimate the wind energy input to the surface waves in the World Ocean (Table 1). For example, the spatial distribution of energy input calculated from (2) and (7) and the latitudinal distribution are shown in Fig. 3. It is clear that the major site of energy input is within the Antarctic Circumpolar Current, which consists of more than 50% of the total input. In addition, the storm tracks in the Northern Hemisphere are also major sites of wind energy input.

As a next step, the wind energy input over the past 54 yr (1948–2002) is examined. Energy input distribution among different frequencies is calculated from (11) and assuming $A = 3.5$ (Fig. 4). There are clearly four peaks, corresponding to periods of 1, 1/2, 1/3, and 1/4 yr, with energy input of 1.50, 0.20, 0.03, and 0.01 TW. In comparison, the rate of energy input corresponding to the mean wind stress is 38.4 TW. The total energy input averaged over the past 54 yr is 52.8 TW, which is noticeably smaller than the values obtained for the time period of July 1997–June 2002.

Wind energy input to the surface waves increases about 20% over the past 50 yr (Fig. 5). Although such an increase may be partially due to the systematic errors induced by the introduction of new instruments, the general trend of increase may be related to wind stress, especially after 1976, which is clearly related to the systematic change in the atmospheric circulation.

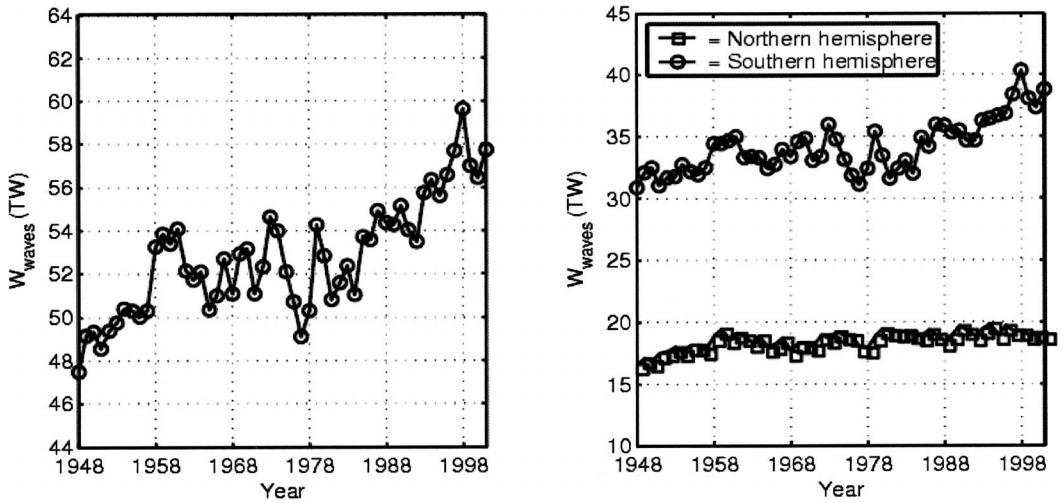

FIG. 5. Interannual variability of wind stress work on the surface waves for (left) global ocean and (right) both hemispheres (TW), calculated from (11).

Most of the energy input is through the Southern Hemisphere, which consists of 2/3 of the total input, while the energy input into the Northern Hemisphere is about 1/3. In addition, the interannual variability of the energy input in the Southern Hemisphere is relatively large.

4. Conclusions

Three estimates of energy input to surface waves, based on an empirical formula and numerical simulations, gave similar results. Thus, a tentative conclusions is that the total amount of wind energy input through surface waves is about 60 TW (for the time period 1997–2002). These estimates are preliminary in nature; however, this study will serve as a first step toward a more accurate balance of the mechanical energy in the World Ocean.

Energy input through the surface waves is at least 20 times that through the surface Ekman drift and the geostrophic current. However, this result does not necessarily mean energy input through the surface waves is the dominating term of mechanical energy supporting gravitational potential energy in the World Ocean.

Most mechanical energy input in surface waves may be dissipated within the surface layer of the oceans through wave breaking, and only a small fraction may be transferred to other forms and locations by the mechanisms of wave–wave interaction and wave–current interaction. Because total energy flux is huge, the energy transferred to other forms is not negligible when compared with other energy sources like wind stress to geostrophic current and Ekman drift, and so on, which will contribute to mixing of the global oceans. Long surface waves may transfer energy generated by local wind stress into remote sites where dissipation can be much stronger, such as beaches. However, the balance of the surface energy on the local scale remains one of the most challenging questions.

Acknowledgments. Author WW was supported by the National Nature Science Foundation of China through Grant 49976003. RXH was supported by the National Science Foundation through Grant OCE-0094807 to the Woods Hole Oceanographic Institution. Reviewers' comments helped to produce a concise and accurate presentation.

REFERENCES

Alford, M. H., 2003: Improved global maps and 54-year history of wind-work on ocean inertial motions. *Geophys. Res. Lett.,* **30**, 1424, doi:10.1029/2002GL016614.

Craig, P. D., and M. L. Banner, 1994: Modeling wave-enhanced turbulence in the ocean surface layer. *J. Phys. Oceanogr.,* **24,** 2546–2559.

Drennan, W. M., M. A. Donelan, E. A. Terray, and K. B. Katsaros, 1996: Oceanic turbulence dissipation measurements in SWADE. *J. Phys. Oceanogr.,* **26,** 808–815.

Faller, A., 1966: Sources of energy for ocean circulation and a theory of the mixed layer. *Proc. Fifth U.S. National Congress of Applied Mechanics,* Minneapolis, MN, ASME, 651–672.

Gemmrich, J. R., T. D. Mudge, and V. D. Polonchicko, 1994: On the energy input from wind to surface waves. *J. Phys. Oceanogr.,* **24,** 2413–2417.

Lueck, R., and R. Reid, 1984: On the production and dissipation of mechanical energy in the ocean. *J. Geophys. Res.,* **89,** 3439–3445.

Maat, N., C. Kraan, and W. A. Oost, 1991: The roughness of wind waves. *Bound-Layer Meteor.,* **54,** 89–103.

Phillips, O. M., 1977: *The Dynamics of the Upper Ocean.* 2d ed. Cambridge University Press, 336 pp.

Terray, E. A., M. A. Donelan, Y. C. Agraval, W. M. Drennan, K. K. Kahma, A. J. Williams III, P. A. Hwang, and S. A. Kitaigorodskii, 1996: Estimates of kinetic energy dissipation under breaking waves. *J. Phys. Oceanogr.,* **26,** 792–807.

Toba, Y., 1974: Duality of turbulence and wave in wind waves. *J. Oceanogr. Soc. Japan,* **30,** 33–34.

Wang, W., and R. X. Huang, 2004: Wind energy input to the Ekman layer. *J. Phys. Oceanogr.,* **34,** 1267–1275.

Watanabe, M., and T. Hibiya, 2002: Global estimates of the wind-induced energy flux to inertial motion in the surface mixed layer. *Geophys. Res. Lett.,* **29**, 1239, doi:10.1029/2001GL04422.

Wu, J., 1982: Wind-stress coefficients over sea surface from breeze to hurricane. *J. Geophys. Res.,* **87,** 9704–9706.

Wunsch, C., 1998: The work done by the wind on the oceanic general circulation. *J. Phys. Oceanogr.,* **28,** 2332–2340.